

Holographic fabrication of 3D photonic crystals using silicon based reflective optics element

Jeff Lutkenhaus,¹ Franz Aguirre Farro,¹ David George,¹ Kris Ohlinger,¹
Hualiang Zhang,² Zsolt Poole,³ Kevin P. Chen,³ and Yuankun Lin^{1,2,*}

¹Department of Physics, Univ. of North Texas, Denton, TX 76203, USA

²Department of Electrical Engineering, Univ. of North Texas, Denton, TX 76203, USA

³Dept. of Electrical and Computer Engineering, Univ. of Pittsburgh, Pittsburgh, PA 15213, USA

*yuankun.lin@unt.edu

Abstract: We present a silicon based single optical element that is able to automatically generate desired laser beam polarizations and intensities for the holographic fabrication of woodpile-type photonic crystal templates. A polydimethylsiloxane (PDMS) mold based reflective optics element is fabricated for the generation of five-beam interferences where four beams are arranged four-fold symmetrically around a central beam. Silicon chips in the inner surfaces of the mold are used to reflect the circularly or elliptically polarized beam into four side beams that are linearly polarized with electric fields normal to the incident plane, and reduce their laser intensities. Photonic crystal templates are holographically fabricated in a photosensitive polymer through this silicon-on-PDMS based single optical element and single beam based configuration.

©2012 Optical Society of America

OCIS codes: (160.5298) Photonic crystals; (090.2890) Holographic optical elements; (220.3740) Lithography.

References and links

1. J. D. Joannopoulos, R. D. Meade, and J. N. Winn, *Photonic Crystals* (Princeton, 1995).
2. S. Noda, M. Yokoyama, M. Imada, A. Chutinan, and M. Mochizuki, "Polarization mode control of two-dimensional photonic crystal laser by unit cell structure design," *Science* **293**(5532), 1123–1125 (2001).
3. K. P. Chen, B. McMillan, and L. Cashdollar, "Self-heated fiber Bragg grating sensors," *Appl. Phys. Lett.* **86**, 143503 (2005).
4. Y. Liu, F. Qin, Z.-M. Meng, F. Zhou, Q.-H. Mao, and Z.-Y. Li, "All-optical logic gates based on two-dimensional low-refractive-index nonlinear photonic crystal slabs," *Opt. Express* **19**(3), 1945–1953 (2011), <http://www.opticsinfobase.org/oe/abstract.cfm?URI=oe-19-3-1945>.
5. A. Tandaechanurat, S. Ishida, D. Guimard, M. Nomura, S. Iwamoto, and Y. Arakawa, "Lasing oscillation in a three-dimensional photonic crystal nanocavity with a complete bandgap," *Nat. Photonics* **5**(2), 91–94 (2011).
6. K. M. Ho, C. T. Chan, C. M. Soukoulis, R. Biswas, and M. Sigalas, "Photonic band gaps in three dimensions: new layer-by-layer periodic structures," *Solid State Commun.* **89**(5), 413–416 (1994).
7. A. Blanco, E. Chomski, S. Grabtchak, M. Ibisate, S. John, S. W. Leonard, C. Lopez, F. Meseguer, H. Miguez, J. P. Mondia, G. A. Ozin, O. Toader, A. Geoffrey, O. Toader, and H. M. van Driel, "Large-scale synthesis of a silicon photonic crystal with a complete three-dimensional bandgap near 1.5 micrometres," *Nature* **405**(6785), 437–440 (2000).
8. M. Deubel, G. von Freymann, M. Wegener, S. Pereira, K. Busch, and C. M. Soukoulis, "Direct laser writing of three-dimensional photonic-crystal templates for telecommunications," *Nat. Mater.* **3**(7), 444–447 (2004).
9. A. J. Turberfield, M. Campbell, D. N. Sharp, M. T. Harrison, and R. G. Denning, "Fabrication of photonic crystals for the visible spectrum by holographic lithography," *Nature* **404**(6773), 53–56 (2000).
10. S. Yang, M. Megens, J. Aizenberg, P. Wiltzius, P. M. Chaikin, and W. B. Russel, "Creating periodic three-dimensional structures by multibeam interference of visible laser," *Chem. Mater.* **14**(7), 2831–2833 (2002).
11. Y. Lin, P. R. Herman, and K. Darmawikarta, "Design and holographic fabrication of tetragonal and cubic photonic crystals with phase mask: toward the mass-production of three-dimensional photonic crystals," *Appl. Phys. Lett.* **86**(7), 071117 (2005).
12. Y. Lin, A. Harb, D. Rodriguez, K. Lozano, D. Xu, and K. P. Chen, "Fabrication of two-layer integrated phase mask for single-beam and single-exposure fabrication of three-dimensional photonic crystal," *Opt. Express* **16**(12), 9165–9172 (2008), <http://www.opticsexpress.org/abstract.cfm?URI=OPEX-16-12-9165>.

13. D. Chanda, L. E. Abolghasemi, M. Haque, M. L. Ng, and P. R. Herman, "Multi-level diffractive optics for single laser exposure fabrication of telecom-band diamond-like 3-dimensional photonic crystals," *Opt. Express* **16**(20), 15402–15414 (2008), <http://www.opticsexpress.org/abstract.cfm?URI=OPEX-16-20-15402>.
14. K. Ohlinger, H. Zhang, Y. Lin, D. Xu, and K. P. Chen, "A tunable three layer phase mask for single laser exposure 3D photonic crystal generations: bandgap simulation and holographic fabrication," *Opt. Mater. Express* **1**(5), 1034–1039 (2011), <http://www.opticsinfobase.org/ome/abstract.cfm?URI=ome-1-5-1034>.
15. Y. K. Pang, J. C. Lee, C. T. Ho, and W. Y. Tam, "Realization of woodpile structure using optical interference holography," *Opt. Express* **14**(20), 9113–9119 (2006), <http://www.opticsinfobase.org/oe/abstract.cfm?URI=oe-14-20-9113>.
16. D. Xu, K. P. Chen, A. Harb, D. Rodriguez, K. Lozano, and Y. Lin, "Phase tunable holographic fabrication for three-dimensional photonic crystal templates by using a single optical element," *Appl. Phys. Lett.* **94**(23), 231116 (2009).
17. S.-G. Park, M. Miyake, S.-M. Yang, and P. V. Braun, "Cu₂O inverse woodpile photonic crystals by prism holographic lithography and electrodeposition," *Adv. Mater.* **23**(24), 2749–2752 (2011).
18. T. Y. M. Chan, O. Toader, and S. John, "Photonic band-gap formation by optical-phase-mask lithography," *Phys. Rev. E Stat. Nonlin. Soft Matter Phys.* **73**(4), 046610 (2006).
19. O. Toader, T. Y. M. Chan, and S. John, "Diamond photonic band gap synthesis by umbrella holographic lithography," *Appl. Phys. Lett.* **89**(10), 101117 (2006).
20. D. F. Edwards, "Silicon (Si)," in *Handbook of Optical Constants of Solids*, E. D. Palik, ed. (Academic, 1985).

1. Introduction

Photonic crystals (PhCs) are dielectric periodic materials with photonic bandgaps where electromagnetic wave propagation is forbidden [1,2]. Studies of photonic crystals have been driven by their potential applications. One-dimensional PhCs such as fiber Bragg gratings can be fabricated easily for applications in fiber optical communications and fiber sensors [3]. Two-dimensional PhCs can be used for an integrated laser on chip [2] and all-optical circuit [4]. Low threshold lasers in three-dimensional (3D) photonic crystals have been predicted and lasing oscillations have been observed in a 3D PhC nanocavity with the highest quality factor yet achieved (~38,500) with quantum dots [5]. However, large-scale fabrication of 3D PhCs with large photonic bandgaps has been a challenge over the past decade. Several methods have been used for fabricating 3D PhCs, such as e-beam lithography for layer-by-layer structures [6], self-assembly of colloidal PhCs [7], two-photon direct laser writing [8], and laser holographic lithography [9,10].

Holographic lithography can produce 3D PhC templates by recording multi-beam 3D interference patterns in a positive or negative photoresist [9,10]. So far, holographic lithography has been successful in fabricating large-volume PhC templates at sub-micro/nano-scales [9–17]. It is an adaptive method because the structure and symmetry of 3D PhC templates can be controlled by the beam propagating directions, the number of the interfering beams, the beam intensities, their respective polarizations, and their relative phases [18,19]. Among various structures, diamond-like and the related woodpile structures have been intensively studied because of their wide and robust photonic bandgaps [18,19]. However, optical alignment is very complicated if bulky mirrors, polarizers, and beam splitters are used in multiple-beam holographic lithography [9,10]. Very recently, a single diffractive [11–14] or reflective [15–17] optical element has been used for laser holographic fabrication of 3D PhC structures in order to reduce the complexity of the optical setup and improve the optical stability. A flat-top prism and multi-layer phase mask have been demonstrated to fabricate diamond-like PhC templates by introducing a phase difference among the diffracted beams [12–19]. Using a flat-top prism, our previous paper has fabricated a woodpile PhC template by introducing a phase shift π of a single side beam relative to others using a glass cover slip as a phase modulation [16]. Other groups have demonstrated a realization of woodpile PhC templates by shifting two counter-propagating side beams by $\pi/2$ relative to the others using the prism [17]. Although both methods have succeeded in the fabrication of large scale 3D PhCs, the control of intensity ratios among the five beams were not considered. Pang et al. have used the flat-top prism to overlap four linearly polarized side beams arranged symmetrically around a circularly polarized central beam [15]. The polarization of each beam has been adjusted individually using wave plates mounted before the flat-top prism.

In this paper, we report a single-beam and single-optical-element based holographic process where the desired polarization and intensity ratio can be easily generated for the fabrication of woodpile-type PhCs. A PDMS mold is used for the generation of four side beams surrounding a central beam. Four silicon chips attached to the PDMS inner surfaces are able to control the polarization of side beams, and reduce their intensities relative to the central beam. 3D woodpile-type PhC templates are fabricated using the PDMS and silicon based reflective optics element.

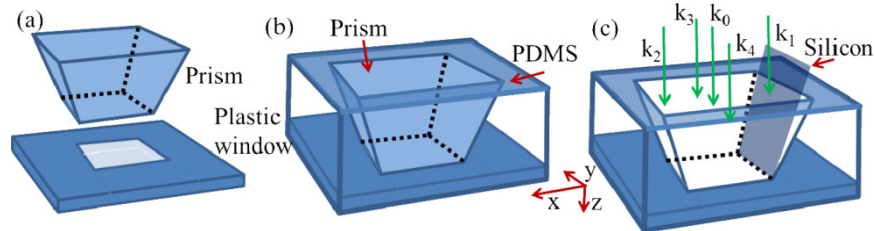


Fig. 1. Schemes of single optical element fabrication: (a) flat-top is supported by a plastic window; (b) PDMS mold is formed surrounding the prism; (c) the prism is removed and silicon chip is placed on the inner surface of the PDMS mold.

2. Reflective optical element for the generation of woodpile-type 3D structures and theoretic description of five-beam interference

The flat-top prism has been used for the generation of five beam interference patterns [16]. We use the same prism that was used in our previous work [16] for the fabrication of the PDMS mold. The prism was sitting on a plastic base for a mold transfer as shown in Fig. 1(a). Both of them were located inside a container. A pre-polymer solution of PDMS (Dow Corning® Sylgard 184) was prepared by mixing 4.56 g of curing agent with 45.5 g Sylgard polymer. The pre-solution was poured into the container. After the bubbles were blown away, the pre-polymer was cured on a hot-plate at 130 °C for 90 minutes as shown in Fig. 1(b). The prism was then removed and a silicon chip was placed on the inner surface of the PDMS mold with polished sides to reflect the laser beam as shown in Fig. 1(c). A single laser beam can be separated into five beams by such a single optical element with four side beams arranged symmetrically around the central beam. Thin gaps can be formed between these silicon facets, when they are set in the mold. The scattering or diffraction due to these gaps will affect the interference exposure process. For the best results, an aperture made of black aluminum foils can be used to block the beams above these gaps.

The incident angle of laser beams on the silicon surface is 78 degrees. For a laser beam with wavelength 514.5 nm, the silicon refractive index is 4.225 [20]. The amplitude reflection coefficients are -0.05 and -0.9 from beams with polarizations parallel with (p-polarized) and normal to (s-polarized) the incident plane, respectively. The reflectance is 0.25% and 81% for the p-polarized and s-polarized beams, respectively. If the incident beam is circularly polarized, the theoretical reflectance is thus 40.6%. 99.7% of the reflected beam is s-polarized when the circularly polarized beam is incident onto the silicon, and the intensity of the p-polarized beam can be ignored. In our experimental setup, the linearly polarized laser passed through a $\lambda/4$ wave plate. After the wave-plate, the laser beam was elliptically polarized with an ellipticity of 1.28. As shown in Fig. 1(c) for the incident laser beam k_0 propagating in the z direction with the original polarization in the x direction and passing the wave-plate, the measured reflectance is 35.6%, 35.6%, 44.9%, and 44.9% for beams k_1 , k_2 , k_3 , and k_4 , respectively. By passing the laser beam through a polarizing beam-splitting cube, we can improve the laser polarization ratio and produce a perfect circularly polarized laser beam.

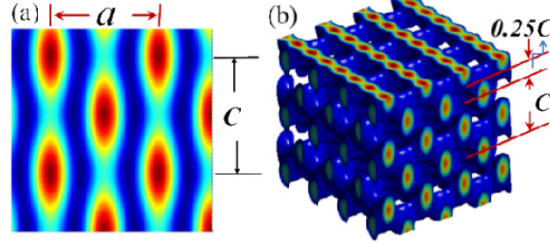


Fig. 2. (a) Three beam interference pattern; (b) Five-beam interference pattern. The interference pattern is shifted by $0.25c$ due to the phase delay.

After passing the single reflective optical element, the formed four side beams and one central beam can be written as (assuming a same initial phase for all side beams),

$$\mathbf{E}_0(\mathbf{r}, t) = \mathbf{E}_{0x} \cos((k_0 \cdot \mathbf{r} - \omega t) + \mathbf{E}_{0y} \cos((k_0 \cdot \mathbf{r} - \omega t + \pi/2), \quad (1)$$

$$\mathbf{E}_1(\mathbf{r}, t) = \mathbf{E}_{1y} \cos((k_1 \cdot \mathbf{r} - \omega t + \delta), \quad (2)$$

$$\mathbf{E}_2(\mathbf{r}, t) = \mathbf{E}_{2y} \cos((k_2 \cdot \mathbf{r} - \omega t + \delta), \quad (3)$$

$$\mathbf{E}_3(\mathbf{r}, t) = \mathbf{E}_{3x} \cos((k_3 \cdot \mathbf{r} - \omega t + \delta), \quad (4)$$

$$\mathbf{E}_4(\mathbf{r}, t) = \mathbf{E}_{4x} \cos((k_4 \cdot \mathbf{r} - \omega t + \delta), \quad (5)$$

where k and ω are the wave vector and angular frequency of the beam, respectively, E is the constant of electric field strength, and δ is the initial phase of the beam. Wave vectors of these five beams can be written as $\{k_0, k_1, k_2, k_3, k_4\} = 2\pi/\lambda\{[0, 0, 1], [\sin \theta, 0, \cos \theta], [-\sin \theta, 0, \cos \theta], [0, -\sin \theta, \cos \theta], [0, \sin \theta, \cos \theta]\}$, where λ is the wavelength of the laser ($\lambda = 514.5$ nm) and θ is the angle between four side beams and central beam.

When these five beams overlap, an interference pattern will be formed, which is determined by the following equation:

$$I(r) = I_0 + \Delta I(r) = \langle \sum_{i=1}^5 E_i^2(r, t) \rangle + \sum_{i < j} E_i \cdot E_j \cos[(k_i - k_j) \cdot r + (\delta_i - \delta_j)] \quad (6)$$

Due to the orthogonal polarization between beams (k_1, k_2) and beams (k_3, k_4), this five-beam interference can be treated as two parallel three-beam interferences. Two sequential overlaps of three-beam interference have been experimentally demonstrated for woodpile-type 3D structures in one of authors' previous works [11]. The interference part of Eq. (6) can be written as a sum of two terms:

$$\sum_{i < j} E_{ix} \cdot E_{jx} \cos[(k_i - k_j) \cdot r + \delta] \quad (7)$$

$$\sum_{p < q} E_{py} \cdot E_{qy} \cos[(k_p - k_q) \cdot r + \frac{\pi}{2} + \delta] \quad (8)$$

Each term can have an interference pattern as shown in Fig. 2(a) but the orientation is rotated by 90 degrees. Furthermore, the phase in Eq. (8) can be written as $(k_p - k_q) \cdot r + \frac{\pi}{2} + \delta = (k_p - k_q) \cdot (r + r_d) + \delta$ where $(k_p - k_q) \cdot r_d = \pi/2$. Thus $r_d = (0.25 a, 0, 0.25c)$ is the shift of interference (among beams k_0, k_1 and k_3) due to the phase delay, where a and c are the lattice constants in x (or y) and z directions, respectively. The interference pattern due to two parallel

three-beam interferences is shown in Fig. 2(b). The shift of pattern in one direction relative to the other is clearly observed and the formed pattern is a woodpile-type structure.

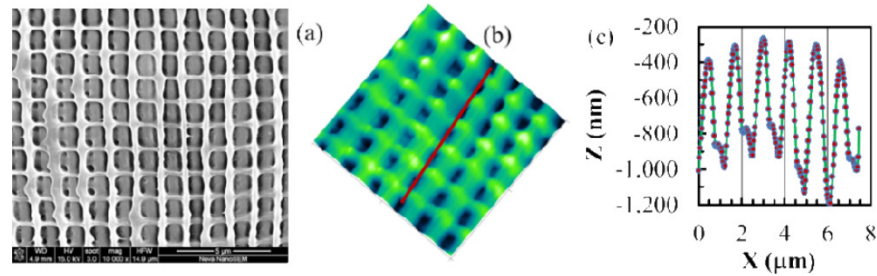


Fig. 3. (a) SEM image of holographically formed 3D photonic crystal template in DPHPA; (b) AFM image of the photonic crystal template in DPHPA; (c) A surface profile measured along the line in the AFM image.

3. Holographic fabrication of 3D photonic structures using the single reflective optical element

An Ar ion laser beam (514.5 nm, Coherent Inc.) was passed through a quarter wave plate and spatial filter, expanded and collimated to a size of 2 inches. The photoresist was a mixture of the following components in the specified weight concentrations: dipentaerythritol penta/hexaacrylate (DPHPA) monomer (Aldrich, 90.36%), a photo initiator rose bengal (0.16%), co-initiator N-phenyl glycine (NPG, 0.67%), and chain extender N-vinyl pyrrolidinone (NVP, 8.81%). The mixture was spin-coated on a glass slide with a speed of 600 rpm for 30 seconds. The photoresist film was exposed to the interference pattern formed through the single beam and the single reflective optical element. The laser power was 200 mW, and a typical exposure was 1.2 seconds. In a mixture batch where the weight concentration of Rose Bengal was reduced by half, a power of 260 mW was then used. The exposed sample was developed in PGMEA for 3 minutes, rinsed by isopropanol for one minute and left to dry in air.

Figure 3(a) shows a scanning electron microscope (SEM) image of the holographically formed 3D photonic crystal template in DPHPA. The SEM image shows a woodpile-like structure and looks similar to the simulated interference pattern in Fig. 2. Based on the scale bar on the SEM, the lattice period in the x (or y) direction is measured to be 1.239 microns. Figure 3(b) shows an atomic force microscope (AFM) image of the 3D photonic crystal template in DPHPA. A surface profile along the line in the AFM is shown in Fig. 3(c) and the lattice period in the x-direction is measured to be 1.232 microns. The lattice constant in the x (or y)-direction is 1.248 microns based on a theoretical calculation for an incident angle of 78 degrees. The agreement between measured and theoretical values is very good.

4. Interference angle reconfiguration for the holographic fabrication of 3D structures

The above multi-beam interference with 78 degree incident angle (which is close to the Brewster angle) can only generate tetragonal photonic crystals [11]. In order to improve the crystal symmetry, thus increasing the photonic bandgap size, the incident angle needs to be changed. For the incident angle of 54.7 degrees (for example), the interfering angle between side beam and central beam is 70.5 degrees thus a face-centered cubic crystal can be generated. When the incident angle is decreased from 78 to 54.7 degrees, the reflectance for p-polarized beam is increased from 0.25% to 18% and for s-polarized beam the reflectance is decreased from 81% to 60%. The interference patterns are still dominated by the interference between the central, circularly-polarized beam and the side, s-polarized beam. However, a deviation from the ideal p-polarization will influence the symmetry of the PhC and the motif in the unit cell of the PhC. When the incident angle is decreased, the lattice constant c/a (c and a are lattice constants in the z and x -directions, respectively) will change [11,14]. A

compromise among the crystal symmetry, the beam intensity ratio and the beam polarization can be made by a comprehensive calculation of bandgap sizes in various formed structures [11,14].

To demonstrate the incident angle reconfiguration capability, we added a piece of glass slide with a thickness of 1 mm under the silicon chip on the bottom edge of the PDMS mold in Fig. 1(c). The incident angle is thus changed from 78 to 74.9 degrees. This new optical element was used for the holographic fabrication of 3D photonic crystal templates. Figure 4(a) shows an AFM image of the 3D photonic crystal template fabricated in DPHPA with a similar experimental condition. A surface profile is shown in Fig. 4(b) for the lined section in the AFM image. Woodpile-like structures are clearly visible. The lattice period in the x-direction is measured to be 1.023 micron from the surface profile, in good agreement with the theoretical value of 1.024 microns. The crystal symmetry is improved because the AFM tip can get more information of structures in the z-direction when the lattice constant in the z-direction is decreased.

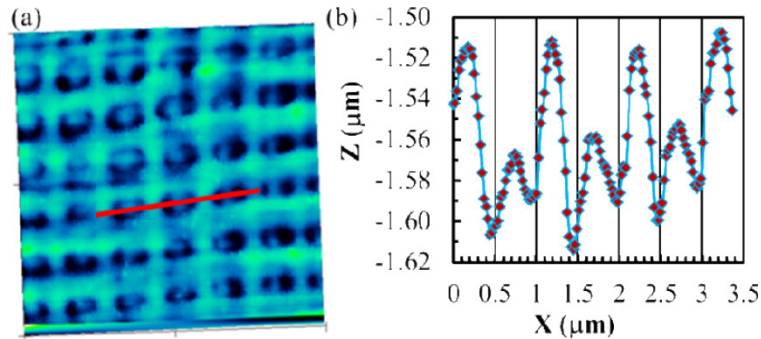


Fig. 4. (a) AFM image of the photonic crystal template in DPHPA fabricated with the incident angle of 74.9 degrees; (b) A surface profile measured along the line in the AFM image.

Using the flat-top prism, all five beams have the same intensity assuming the incident beam is uniform [16,17]. Using the current single silicon based reflective optical element, the ratio of the central beam intensity over the side beam intensity is around 2.5. The intensity contrast in the interference pattern is improved comparing the current optical element with the flat-top prism (the best ratio is 4 for the five-beam interference [19]). The improved intensity contrast can help remove un-polymerized monomers out of the 3D polymerized interconnected structures during the development process.

5. Conclusion

A silicon based reflective optical element can be used to generate and steer multi-beams, change their polarizations and intensity ratios for the holographic fabrication of woodpile-like 3D photonic structures. 3D photonic crystal templates have been fabricated in DPHPA using such a single optical element and single exposure process.

Acknowledgments

We thank David Garrett for collecting SEM images for us. This work is supported by research grants from the U.S. National Science Foundation under Grant Nos. CMMI-0900564, DMR-0934157, CMMI-1109971 and ECCS-1128099.